Available online at www.sdcjter.in

SDC Journal of Theoretical and Experimental Research (SDCJTER) 01(01), 2023, 16–25

Optical Properties of Zn doped SnS Nanoparticles

K.T. Ramla[a, b], S.B. Rakesh Chandran [c] and A. P. Sunitha[a*]

[a] *Department of Physics, Government Victoria College, Palakkad, Kerala-678001*
[b] *P. T. M. Government College, Perinthalmanna, Malappuram, Kerala-676552*
[c] *Department of Physics, Sanatana Dharma College, Alappuzha, Kerala, India, 688 003*

Available online 01January 2023

Abstract

Tin sulphide (SnS) nanoparticles and Zinc (Zn) doped SnS nanoparticles were synthesized by ~~a~~ cost-effective wet chemical method. Doping SnS with Zn was done at various wt. percentages. To analyze the optical properties of as synthesized materials UV-Vis-NIR absorption studies and photoluminescence studies were conducted. The samples were characterized by X-Ray diffraction, and dynamic light scattering experiments for structural and size analysis. Sn*S and Zn-dopedSnS exhibit wide absorption from UV-visible to near IR region suggesting the potential application of Zn doped SnS as an absorber layer in photovoltaic applications. 3 wt.% Zn doped SnS attains maximum crystallinity, absorbance and photoluminescence whereas for higher and lower concentrations it shows the reduction in performance.

Keywords: SnS nanoparticles; doping; Zn doped SnS; wet chemical method

1. Introduction

Nowadays research is mainly focusing on the preparation of non-toxic nanoparticles for various energy applications. Tin monosulphide is the only naturally occurring member of the Group IV-VI monochalcogenides[1]. SnS is a promising material for semiconducting and optical applications because it is earth-abundant, non-toxic and eco-friendly material with a large absorption coefficient and high carrier concentration [2], [3]. Other members of Group IV-VI monochalcogenides such as PbS and PbSe are potential materials for solar cell applications but they contain hazardous elements which produce severe health issues for humans and the environment [4]. The optical band edge determines the optical property of SnS and changes with size, shape and doping [5]. SnS has an inert surface because of the absence of dangling bonds and Fermi-level spinning between SnS layers. SnS crystal has a layered structure, in which the atoms of the same layer are connected by strong covalent bonds and the inter-layer atoms are bonded by weak van der Waals forces which easily lead to 2D morphologies [6].The lattice constants are a = 4.31Å, b = 11.39 Å and c = 3.98 Å with orthorhombic structure [7].

SnS possess both direct and indirect bandgap which makes it a promising material for applications in solar cells and NIR detectors [8-10]. SnS is a good candidate for bioimaging since

* Corresponding author: *Email address*: *sunithaganesh@gvc.ac.in* (A.P Sunitha)

the absorption and emission peaks in the NIR region [11]. Absorption in the visible region was found to be increased by introducing SnS QDs into sensitized TiO_2 solar cells [12]. Black phosphorene is a material with the potential optoelectronic application but it lacks stability. Tin mono sulphide is analogous to black phosphorene which shows better stability [13].The intense anisotropic behaviour of SnS strongly influences the electronic nature of the compound. SnS is a material with p-type activity due to Sn deficiencies having a direct gap of 1.2-1.5 eV most suited to solar spectrum and indirect band gap 1.1 eV with carrier concentration around 10^{17}-10^{18} /cm^3, high optical absorption coefficient >10^4 /cm and high conversion efficiency (25%) which is suitable for photovoltaic applications [14-17].

The addition of impurities to SnS can produce changes in structural, morphological, optical and electronic properties [17-19]. An acceptor impurity improves the photovoltaic performance of SnS[20]. Hosein et al performed Se doping in SnS and the doping improved the crystallinity and optical properties of the material [21]. Wang et al synthesized SnS: Ce^{3+} by chemical deposition method and the band gap is found to be decreased with the increase in doping concentration and the photoluminescence also increases with an increase in doping [22]. Indium-doped SnS exhibited improved performance for solar cell applications and the dopants enhances the optical performance by introducing an additional energy level in the electronic band structure and the band gap is maximum for lesser concentration [23]. Doping by Nd improves the transmittance of SnS along with an increase in bandgap[24].

Pandey et al studied the effect of various buffer layers on the performance of SnS for solar cell applications [25]. SnS/PVP core/shell QDs helped to tune the emission colour from blue to orange and a low concentration of PVP provided better stability to SnS QDs [26]. Doping by sodium provided a wide range of carrier concentrations and better thermoelectric performance [27]. Doping SnS by Al revealed a reverse effect in optical transmittance and bandgap[28].SnS thin film grown on ZnO substrate can act as a window layer in solar cells [29]. The maximum solubility of Ge in SnS is obtained at 6 at. % and the band gap can be tuned in the range of 1.25-1.35 eV by altering the concentration [30]. Anis et al synthesized Cu doped SnS and the optimum doping concentration is obtained at 6 % for the absorption coefficient of the order of $2x10^6$ cm^{-1}[19]. In the present work, we report a simple and cost-effective method for synthesizing SnS nanoparticles and also Zn-doped SnS nanoparticles with non-toxic precursors in water-based solutions and investigate their structural and optical properties.

2. Experimental Section

2.1. Synthesis of SnS Nanoparticles

The precursors used for the synthesis are $SnCl_2$, $ZnCl_2$ and Na_2S. 4.513 g of $SnCl_2.2H_2O$ and 1.561 g of Na_2S were separately dissolved in 50 ml of deionized water to prepare a 0.4 M solution of each. Na_2S solution was added to the Tin chloride solution dropwise with constant stirring. A dark brown solution was obtained immediately after mixing the precursor solutions. The solution was stirred continuously by a magnetic stirrer at 400 rpm for 2 hours at room temperature. The mixture was then centrifuged at 2000 rpm for 10 minutes. The precipitate was washed several times by using Isopropyl alcohol and deionized water. After that, the solution was dried in a hot air oven at 80 ^{0}C and obtained in a powder form. The powdered SnS (sample-S1) was grinded for about 1 hour in a mortar.

2.2. Synthesis of Zn Doped SnS Nanoparticles

0.061 g of $ZnCl_2$ (1 wt. Percentage) was added to the mixture of 0.4 M solution of Tin Chloride and Na_2S.The solution was processed to get a powder form of Zn doped SnS nanoparticles (sample-S2). Different samples were prepared by adding 0.122 g,0.183 g,0.244g,0.305 g of $ZnCl_2$ to the mixture of tin chloride and Na_2S and kept as samples S3, S4, S5, S6 respectively.

The undoped sample (S1) and 1 wt. Percentage doped samples (S2) were characterized by a Dynamic Light Scattering instrument (Horiba Scientific SZ-100) to get the size of the particles. X-Ray diffraction analysis (Cu-Kα-XRE with wavelength 1.540598 A^0)was conducted for material characterization. To analyze the optical properties of as synthesized samples absorption studies were conducted with DT-3000 absorption spectrometer and photoluminescence studies were conducted with LSR-PS-113 emission spectrometer.

3. Experimental Results

3.1 Dynamic Light Scattering

The Dynamic Light Scattering (DLS) was performed at a measurement Gate Time of 80 ns. DLS gives the distribution of particles according to the particle size. The histogram showing the size distribution of SnS nanoparticles is shown in Fig. 1. DLS measurement confirms that the prepared sample contains particles in the nano regime.

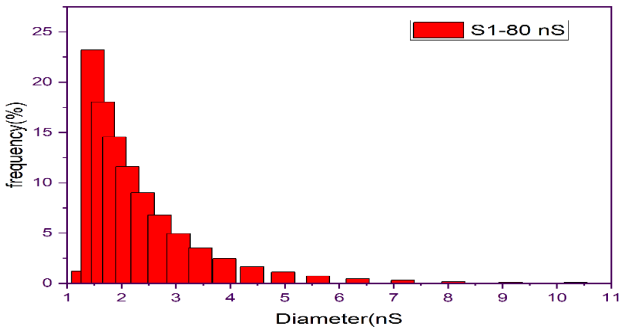

Fig.1. Histogram showing the distribution of undoped SnS nanoparticles

3.2 XRD analysis

Powder XRD pattern of the samples are shown in Fig. 2(a) (b) and (c). The XRD pattern of sample 1 (S1) confirmed the pure crystalline and orthorhombic phase of SnS. A high-intensity diffraction peak is observed at 31.7 ^{0} which indicates that the SnS nanostructures are preferentially oriented along the (1 1 1) plane. The preferential direction is the result of controlling the growth process by nucleation [31]. SnS with (1 1 1) plane shows maximum efficiency in SnS based solar cells and photovoltaic applications [32]. The other major peaks are obtained at 26.4 ^{0},39.01 ^{0}, and 51.05 ^{0}respectively corresponding to the planes (1 2 0), (1 3 1), and (1 1 3) respectively.

The peaks are indexed with the pure orthorhombic phase of SnS corresponding to JCPDS Card No:75-0925 [7].

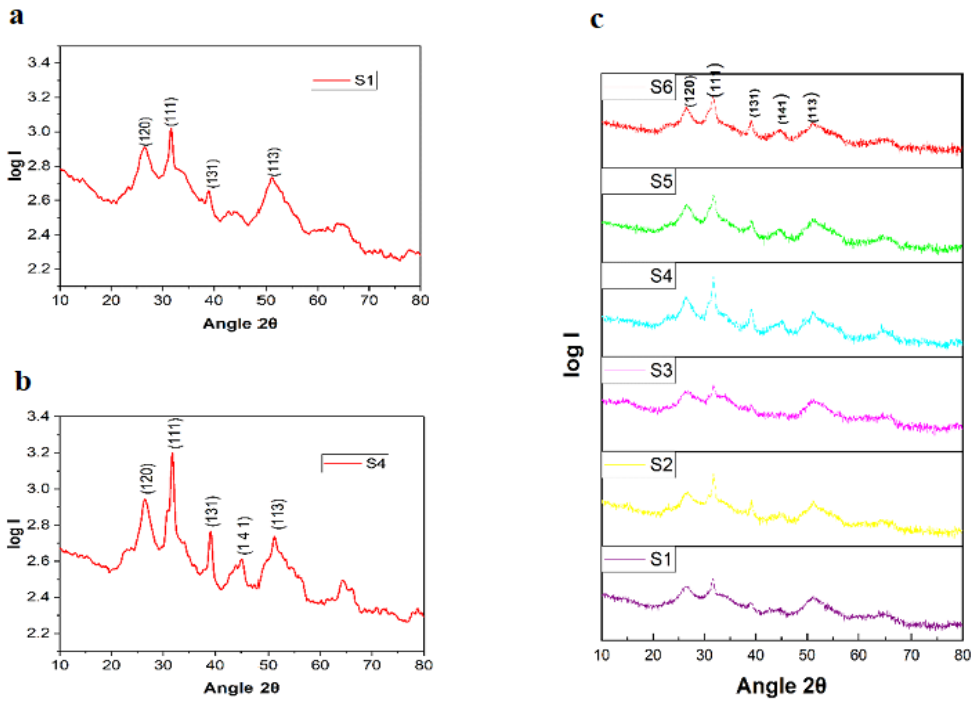

Fig.2. XRD patterns of (a) undopedSnS nanoparticles (b) 3 wt.% Zn doped SnS (c) undopedSnS,1wt.%,2 wt.%,3 wt.%,4wt.% and 5wt.% Zn doped SnS nanoparticles.

XRD patterns of Zn doped samples show similar peaks but as the doping increases the diffraction peaks of XRD were also found to be increased. The maximum intensity and sharp diffraction peak are obtained at 3 wt.% doping. The increased diffraction peak indicates the enhanced crystallinity and can probably be due to the creation of new nucleating centers from dopants which favours the growth of SnS [33]. The reduction in XRD peak at higher concentration is due to the incorporation of more Zn atoms into the SnS lattice and can also be attributed to increased stacking defects due to the change in ionic radius of Zn^{2+} and Sn^{2+} ions leading to the loss of periodicity in the SnS lattice arrangement [17], [31]. The nucleation centers attain their saturation at higher concentrations [33]. The high-intensity diffraction peak corresponds to the preferential orientation plane along the (1 1 1) plane. The other major peaks are obtained corresponding to the planes (1 2 0), (1 3 1), (1 4 1), and (1 1 3) respectively which corresponds to the orthorhombic phase of SnS. No separate peaks were obtained which indicates that Zn^{2+} has successfully replaced Sn^{2+} in SnS nanoparticles and also the pure phase of SnS [16], [31]. The morphology and structure of pure SnS nanoparticles and Zn-dopedSnS nanoparticles are similar.

3.3 Optical properties

The absorbance of SnS nanostructure as a function of wavelength is shown in figure 3(a)-(f). The characteristic absorption peak of SnS nanostructure is obtained in the UV region which is due to the transition of electrons from the valence band to the conduction band [3]. As synthesized SnS nanostructure exhibited wide absorption in the UV-visible to near IR region which indicates that it can be used for the absorption of sunlight [34], [35]. Zn-dopedSnS nanoparticles exhibited wide absorption from UV-visible to near IR region with an absorption peak in the UV region. Absorption is found to vary with doping. The absorbance is higher in the case of 3 wt. Percentage Zn doped SnS. Further increase in doping decreases the absorbance. It can be seen that Zn doping can affect the absorption ability of SnS. The maximum absorption ability was obtained for sample S4 which is the 3-wt. percentage Zn-dopedSnS nanoparticles.

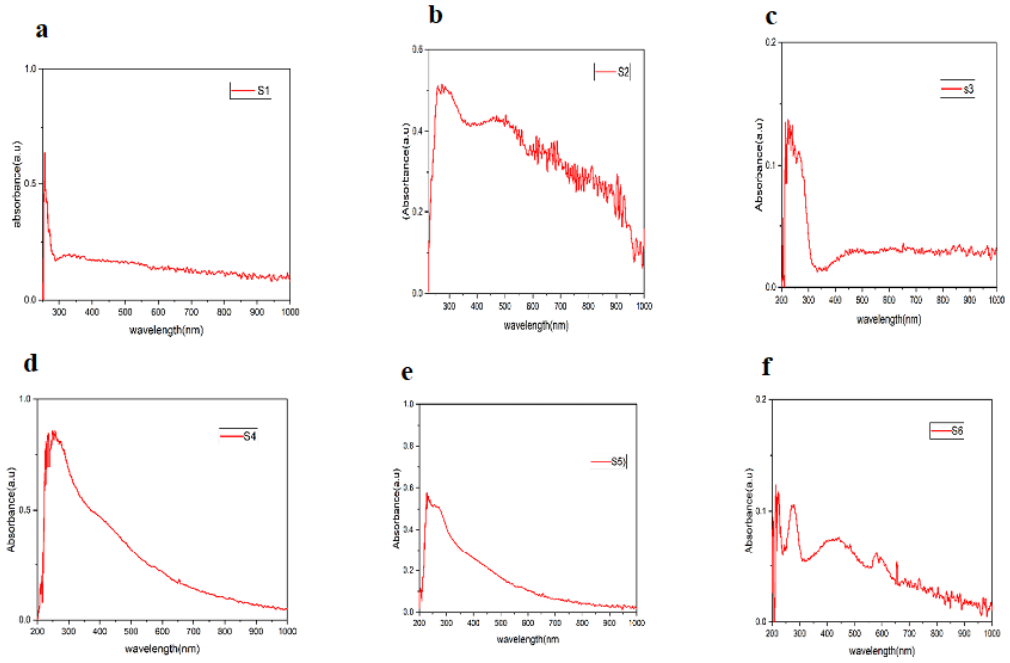

Fig.3. Absorption spectrum of undopedSnS and Zn doped SnS nanoparticles (a) undopedSnS (b) 1 wt.% Zn doped SnS(c) 2wt % Zn doped SnS (d) 3 wt.% Zn doped SnS (e)4 wt.% Zn doped SnS (f) 5 wt.% Zn doped SnS

Photoluminescence studies were conducted using two excitation sources blue and green of wavelength 435 nm and 511nm respectively. Figure.4(a)-(f) is the photoluminescence spectra of SnS and Zn doped SnS with excitation wavelength 435 nm. A strong green emission is obtained. The photoluminescence shows variation with the level of doping. As the doping increases photoluminescence peak is found to be increasing and when the doping become 3 wt. Percentage PL shows a maximum peak. The same sample exhibited a maximum peak in the absorption spectrum. Further increase in doping decreases the photoluminescence peak. This can be attributed to a concentration quenching phenomenon [22] This is because as the concentration of doped Zn^{2+} increases, there will be a charge imbalance in the crystal and which produces trapping centres within the crystal. This could lead to cross-relaxation and non-radiative transition and reduces the photoluminescence efficiency. This trend in photoluminescence is reported in

studies[10,31]. The optimum value of doping is found in sample S4 which is 3 wt. percentage Zn doped SnS.

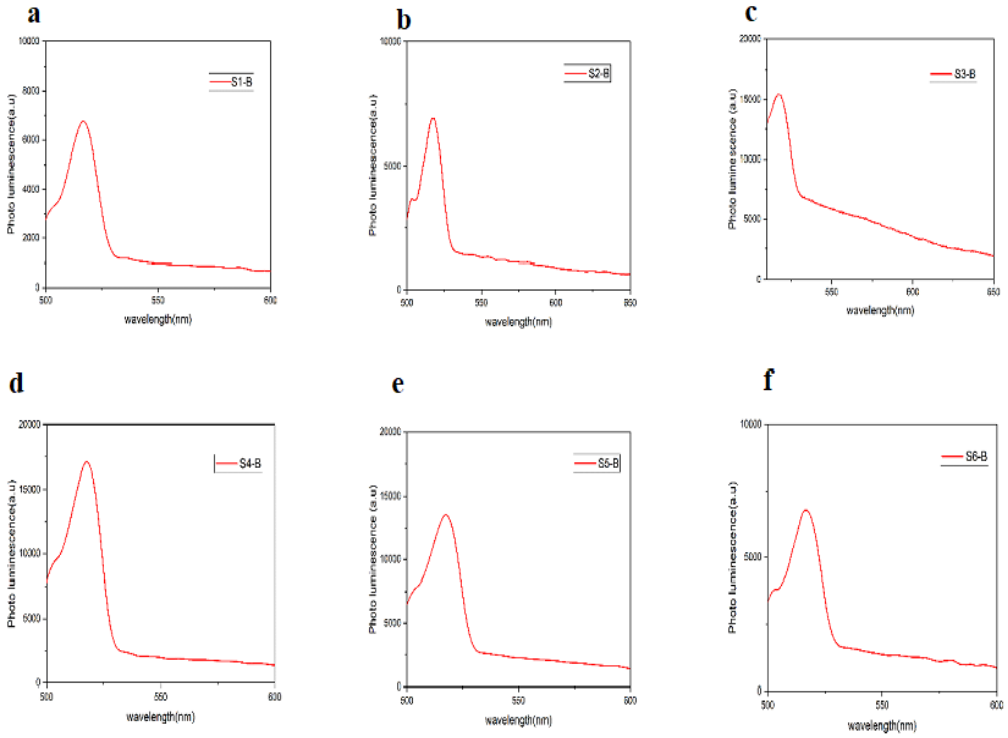

Fig.4.Photoluminescence spectra using a blue excitation wavelength of (a) undopedSnS (b) 1 wt.% Zn doped SnS (c) 2 wt.% Zn doped SnS (d) 3 wt.% Zn doped SnS (e) 4 wt.% Zn doped SnS (f) 5 wt.% Zn doped SnS nanoparticles

Figure. 5(a)-(f) is the PL spectra with excitation wavelength 511 nm. An increase in the level of doping increases the photoluminescence intensity up to 3-wt. percentage and a further increase in doping decrease the PL intensity. The intensity variations can be due to the density of free excitons and the concentration quenching phenomenon [24]. The maximum PL peak corresponds to the 3-wt. percentage Zn-doped SnS nanoparticles. Further increase in doping results in the decreased efficiency of photoluminescence, which is the optimum level of doping for maximum photoluminescence, which indicates that the optimum doping with Zn improves the optical properties of SnS nanoparticles.

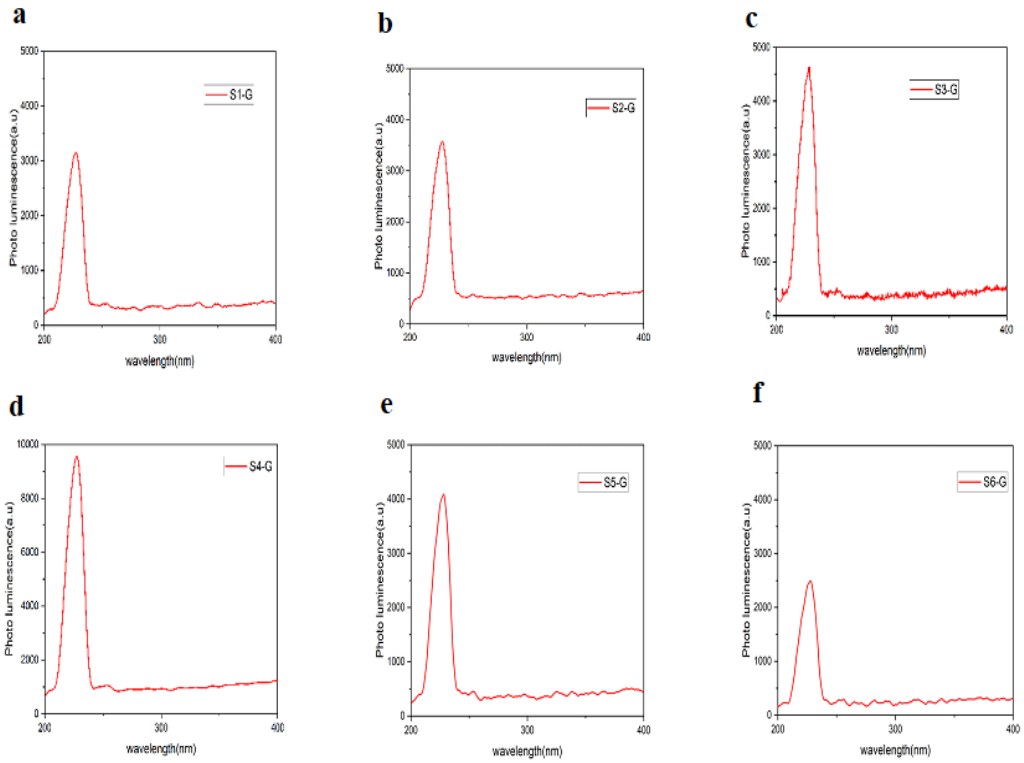

Fig.5.Photoluminescence spectra using green excitation wavelength (a) undopedSnS (b) 1 wt. %Zn doped SnS (c) 2 wt.% Zn doped SnS (d) 3 wt.% Zn doped SnS (e) 4 wt.% Zn doped SnS (f) 5 wt.% Zn doped SnS nanoparticles

4. Conclusion

Without using any toxic chemicals SnSnanocrystals and Zn-doped SnSnanocrystals were synthesized by using the wet chemical method. The majority of the particles synthesized were in the range of 13-21 nm. XRD analysis confirmed the orthorhombic nature and the preferential orientation is found to be along the (1 1 1) plane. The prepared nanoparticles show a wide absorption range from UV-visible to near IR region. Greater absorbance, maximum intensity Pl peaks, and the high intensity in the XRD pattern is obtained in the 3-wt. percentage Zn doped SnS nanoparticles.3 wt. % Zn doped SnS is the optimum level of doping for improved optical performance. Properties of Zn doped SnS synthesized at optimum conditions are suitable for use in absorber layers for solar cell applications.

Acknowledgments

The authors would like to acknowledgeDr. K J Saji, International School of Photonics, CUSAT, Kochin-22 for providing DLS facilities, DST, FIST Govt. Victoria College, Palakkad for providing the instrumentation facilities.

References

Akkari, A., Reghima, M., Guasch, C., & Kamoun-Turki, N. (2012). Effect of copper doping on physical properties of nanocrystallized SnS zinc blend thin films grown by chemical bath deposition. *Journal of Materials Science*, *47*(3), 1365–1371. https://doi.org/10.1007/s10853-011-5912-y

Bhorde, A., Pawbake, A., Sharma, P., Nair, S., Funde, A., Bankar, P., More, M., & Jadkar, S. (2018). Solvothermal synthesis of tin sulfide (SnS) nanorods and investigation of its field emission properties. *Applied Physics A: Materials Science and Processing*, *124*(2). https://doi.org/10.1007/s00339-017-1529-6

Chaki, S. H., Chaudhary, M. D., & Deshpande, M. P. (2015). Effect of indium and antimony doping in SnS single crystals. *Materials Research Bulletin*, *63*, 173–180. https://doi.org/10.1016/j.materresbull.2014.12.013

Cheng, H. Y., Acar, O., Shih, W. Y., & Shih, W. H. (2020). Enhancing the photoluminescence of SnS quantum dots by ZnS treatment. *Chemical Physics Letters*, *754*. https://doi.org/10.1016/j.cplett.2020.137696

Deepa, K. G., & Nagaraju, J. (2012). Growth and photovoltaic performance of SnS quantum dots. *Materials Science and Engineering B: Solid-State Materials for Advanced Technology*, *177*(13), 1023–1028. https://doi.org/10.1016/j.mseb.2012.05.006

Díaz-Cruz, E. B., Regalado-Pérez, E., Santos, J., & Hu, H. (2021). Development of SnS/PVP core/shell quantum dots with tunable color emission synthesized by microwave heating. *Journal of Solid-State Chemistry*, *300*. https://doi.org/10.1016/j.jssc.2021.122264

Ghosh, B., Das, M., Banerjee, P., & Das, S. (2009). Fabrication of the SnS/ZnO heterojunction for PV applications using electrodeposited ZnO films. *Semiconductor Science and Technology*, *24*(2). https://doi.org/10.1088/0268-1242/24/2/025024

Grace Ninan, G., Sudhakartha, C., & Vijayakumar, K. P. (2019). *Synthesis Of Spray Pyrolysed Copper Doped Tin Sulfide (SnS: Cu) Thin Films By Optimizing The Anionic Precursor Molarity*. www.sciencedirect.comwww.materialstoday.com/proceedings

Guo, Y., Shi, W., Zhang, Y., Wang, L., & Wei, G. (2008). Investigations on Sb 2 O 3 doped-SnS thin films prepared by vacuum evaporation. *Sixth International Conference on Thin Film Physics and Applications*, *6984*, 69841Q. https://doi.org/10.1117/12.792636

Han, S., Shih, W. Y., & Shih, W. H. (2017). Charge-Neutral, Stable, Non-Cytotoxic, Near-Infrared SnS Aqueous Quantum Dots for High Signal-to-Noise-Ratio Biomedical Imaging. *ChemistrySelect*, *2*(24), 7332–7339. https://doi.org/10.1002/slct.201700855

Hsu, H. T., Chiang, M. H., Huang, C. H., Lin, W. T., Fu, Y. S., & Guo, T. F. (2015). Effects of Ge-and Sb-doping and annealing on the tunable bandgaps of SnS films. *Thin Solid Films*, *584*, 37–40. https://doi.org/10.1016/j.tsf.2014.10.065

IEEE Staff. (2016). *2016 International Renewable and Sustainable Energy Conference (IRSEC)*. IEEE.

Jamali-Sheini, F., Cheraghizade, M., Niknia, F., & Yousefi, R. (2016). Enhanced photovoltaic performance of tin sulfide nanoparticles by indium doping. *MRS Communications*, *6*(4), 421–428. https://doi.org/10.1557/mrc.2016.48

Kafashan, H., Azizieh, M., & Balak, Z. (2017). Electrochemical synthesis of nanostructured Se-doped SnS: Effect of Se-dopant on surface characterizations. *Applied Surface Science*, *410*, 186–195. https://doi.org/10.1016/j.apsusc.2017.03.062

Koktysh, D. S., McBride, J. R., Geil, R. D., Schmidt, B. W., Rogers, B. R., & Rosenthal, S. J. (2010). Facile route to SnS nanocrystals and their characterization. *Materials Science and Engineering B: Solid-State Materials for Advanced Technology*, *170*(1–3), 117–122.

https://doi.org/10.1016/j.mseb.2010.03.035

Kumar, K. S., Manohari, A. G., Dhanapandian, S., & Mahalingam, T. (2014). Physical properties of spray pyrolyzed Ag-doped SnS thin films for opto-electronic applications. *Materials Letters*, *131*, 167–170. https://doi.org/10.1016/j.matlet.2014.05.186

Li, H., Ji, J., Zheng, X., Ma, Y., Jin, Z., & Ji, H. (2015). Preparation of SnS quantum dots for solar cells application by an in-situ solution chemical reaction process. *Materials Science in Semiconductor Processing*, *36*, 65–70. https://doi.org/10.1016/j.mssp.2015.03.036

Manohari, A. G., Dhanapandian, S., Manoharan, C., Kumar, K. S., & Mahalingam, T. (2014). Effect of doping concentration on the properties of bismuth doped tin sulfide thin films prepared by spray pyrolysis. *Materials Science in Semiconductor Processing*, *17*, 138–142. https://doi.org/10.1016/j.mssp.2013.09.012

Niknia, F., Jamali-Sheini, F., & Yousefi, R. (2016). Examining the effect of Zn dopant on physical properties of nanostructured SnS thin film by using electrodeposition. *Journal of Applied Electrochemistry*, *46*(3), 323–330. https://doi.org/10.1007/s10800-015-0913-1

Nithyaprakash, D., & Chandrasekaran, J. (2010). NLO properties of tin sulfide nanoparticle by precipitation method. In *OPTOELECTRONICS AND ADVANCED MATERIALS-RAPID COMMUNICATIONS* (Vol. 4, Issue 10). https://www.researchgate.net/publication/274195992

Norton, K. J., Alam, F., & Lewis, D. J. (2021). A Review of the Synthesis, Properties, and Applications of Bulk and Two-Dimensional Tin (II) Sulfide (SnS). *Applied Sciences*, *11*(5), 2062. https://doi.org/10.3390/app11052062

Pandey, S., Sadanand, Singh, P. K., Lohia, P., & Dwivedi, D. K. (2021). Numerical Studies of Optimising Various Buffer Layers to Enhance the Performance of Tin Sulfide (SnS)-Based Solar Cells. *Transactions on*

Prastani, C., Nanu, M., Nanu, D. E., Rath, J. K., & Schropp, R. E. I. (2013a). Synthesis and conductivity mapping of SnS quantum dots for photovoltaic applications. *Materials Science and Engineering B: Solid-State Materials for Advanced Technology*, *178*(9), 656–659. https://doi.org/10.1016/j.mseb.2012.10.019

Prastani, C., Nanu, M., Nanu, D. E., Rath, J. K., & Schropp, R. E. I. (2013b). Synthesis and conductivity mapping of SnS quantum dots for photovoltaic applications. *Materials Science and Engineering B: Solid-State Materials for Advanced Technology*, *178*(9), 656–659. https://doi.org/10.1016/j.mseb.2012.10.019

Sarkar, A. S., Mushtaq, A., Kushavah, D., & Pal, S. K. (2020). Liquid exfoliation of electronic grade ultrathin tin (II) sulfide (SnS) with intriguing optical response. *Npj 2D Materials and Applications*, *4*(1). https://doi.org/10.1038/s41699-019-0135-1

Sebastian, S., Kulandaisamy, I., Arulanantham, A. M. S., Valanarasu, S., Kathalingam, A., Jesu Jebathew, A., Shkir, M., & Karunakaran, M. (2019). Influence of Al doping concentration on the opto-electronic chattels of SnS thin films readied by NSP. *Optical and Quantum Electronics*, *51*(4). https://doi.org/10.1007/s11082-019-1812-1

Sebastian, S., Kulandaisamy, I., Arulanantham, A. M. S., Valanarasu, S., Kathalingam, A., Shkir, M., & AlFaify, S. (2022). Enhancement in photovoltaic properties of Nd: SnS films prepared by low-cost NSP method. *Rare Metals*, *41*(5), 1661–1670. https://doi.org/10.1007/s12598-019-01295-2

Sohila, S., Rajalakshmi, M., Ghosh, C., Arora, A. K., & Muthamizhchelvan, C. (2011). Optical and Raman scattering studies on SnS nanoparticles. *Journal of Alloys and Compounds*, *509*(19), 5843–5847. https://doi.org/10.1016/j.jallcom.2011.02.141

Vidal, J., Lany, S., D'Avezac, M., Zunger, A., Zakutayev, A., Francis, J., & Tate, J. (2012). Band-structure, optical properties, and defect physics of the photovoltaic semiconductor SnS. *Applied Physics Letters*, *100*(3). https://doi.org/10.1063/1.3675880

Wang, Z., Qu, S., Zeng, X., Liu, J., Zhang, C., Tan, F., Jin, L., & Wang, Z. (2009). The application of SnS nanoparticles to bulk heterojunction solar cells. *Journal of Alloys and*

Compounds, *482*(1–2), 203–207. https://doi.org/10.1016/j.jallcom.2009.03.158

Wang, M. X., Yue, G. H., Lin, Y. D., Wen, X., Peng, D. L., & Geng, Z. R. (2013). Optical properties and photovoltaic application of the SnS quasi-one-dimensional nanostructures. *Nano-Micro Letters*, *5*(1), 1–6. https://doi.org/10.3786/nml.v5i1.p1-6

Wang, Z., Huang, L. S., Zhang, C., Chuai, M., Zhang, X., & Zhang, M. (2019). The optical properties of Ce-doped SnS quantum dots with fast nanosecond lifetime. *Journal of Alloys and Compounds*, *799*, 425–432. https://doi.org/10.1016/j.jallcom.2019.05.329

Xin, C., Zheng, J., Su, Y., Li, S., Zhang, B., Feng, Y., & Pan, F. (2016). Few-layer tin sulfide: A new black-phosphorus-analogue 2D material with a sizeable band gap, odd-even quantum confinement effect, and high carrier mobility. *Journal of Physical Chemistry C*, *120*(39), 22663–22669. https://doi.org/10.1021/acs.jpcc.6b06673

Yue, G. H., Wang, L. S., Wang, X., Chen, Y. Z., & Peng, D. L. (2009). Characterization and optical properties of the single crystalline SnS nanowire arrays. *Nanoscale Research Letters*, *4*(4), 359–363. https://doi.org/10.1007/s11671-009-9253-6

Zhang, F., Xu, N., Zhao, J., Wang, Y., Jiang, X., Zhang, Y., Huang, W., Hu, L., Tang, Y., Xu, S., & Zhang, H. (2020). Quantum confinement-induced enhanced nonlinearity and carrier lifetime modulation in two-dimensional tin sulfide. *Nanophotonics*, *9*(7), 1963–1972. https://doi.org/10.1515/nanoph-2019-0448

Zhou, B., Li, S., Li, W., Li, J., Zhang, X., Lin, S., Chen, Z., & Pei, Y. (2017). Thermoelectric properties of SnS with na-doping. *ACS Applied Materials and Interfaces*, *9*(39), 34033–34041. https://doi.org/10.1021/acsami.7b08770